Research article

Schmidt number and its influence on turbulent energy dissipation in aeolian sand transport phenomena

Hadjaissa Aissa[1*], **Salameh Tareq Samir Zaki**[2]

[1]Department of Mechanics Engineering, Faculty of Technology, University of Amar Telidji, Algeria
[2]College of Engineering, University of Sharjah, United Arab Emirates
*Corresponding author: a.hadjaissa@lagh-univ.dz

Received: 7 October 2025 - **Reviewed:** 8 November 2025 - **Accepted:** 19 November 2025
https://doi.org/10.17159/caj/2025/35/2.24220

Abstract

This study examines the role of the turbulent Schmidt number (Sc) in shaping the dynamics of aeolian sand transport, with a particular focus on turbulent energy dissipation and particle diffusion. Using a mixture model framework and direct numerical simulations, we investigate both suspension (D = 2 µm) and saltation (D = 250 µm) modes under controlled wind tunnel conditions. Results demonstrate that Sc strongly influences diffusion coefficients and dissipation rates, with a stable convergence identified in the range Sc = 0.7–0.9. This interval represents a physically meaningful threshold where the turbulence structure of air–sand flows remains relatively insensitive to Sc variations. The findings provide not only a refined parameterization of aeolian transport but also a basis for improving predictive models of dust storms, atmospheric pollutant dispersion, and environmental risk assessments. This work highlights the importance of treating Sc as a tunable parameter in environmental fluid dynamics rather than as a fixed constant.

Keywords

Aeolian sand transport, Schmidt number, Mixture model, Turbulent dissipation rate, Particle diffusion

Notations

u: Mixture flow velocity (m/s)
ρ: Mixture flow density (kg/m^3)
D: Diameter of sand particles (m)
μ_t: Viscosity of mixture turbulent (Pa.s)
P: Pressure of mixture flow (Pa)
D_{md}: Turbulent dispersion coefficient (m^2/s)
Cd: Dispersed phase Mass fraction (kg/kg)
u_{slip}: The relative velocity between the two phases (m/s)
τ_{Gm}: Sum of the turbulent viscous stresses (kg/(m·s^2))
α: The interfacial area per unit volume (m2/m3)
n: The number density (1/m^3)
j: The volume-averaged velocity (m/s)
g: The gravitational acceleration (m/s^2)
$Ø_c$: Continuous phase volume fractions (m^3/m^3)
$Ø_d$: Dispersed phase volume fractions (m^3/m^3)
uc: Continuous phase velocity vector (m/s)
ud: Dispersed phase velocity vector (m/s)
ρc: Continuous phase density (kg/m^3)
ρd: Dispersed phase density (kg/m^3)
m_{dc}: Rate of mass transport from the dispersed to the continuous phase(kg/(m^3.s))
Sc: Turbulent Schmidt number
ep: turbulent dissipation rate (m^2/s^3)

Introduction

All terrestrial life forms exist within a fluidic medium, whether it be the atmospheric air or the aquatic environments of rivers, lakes, or oceans. The study of these fluid flows has garnered significant attention over time, leading to the development of distinct disciplines such as meteorology, climatology, hydrology, and hydraulics (Chavez et al., 2011). While the specific objectives of these disciplines, like weather forecasting in meteorology, may foster specialization, environmental concerns necessitate a more holistic approach (Wang et al., 2023). Experts from these fields must collaborate to address interconnected problems, including the effects of turbulence on particles dispersion, interfacial mass and momentum transfer, flow dynamics in complex geometries, and the influence of flow on biological systems (Seinfeld and Pandis, 1997). The study of environmental flows aligns closely with contemporary emphasis on environmental impact assessment and sustainable living (Kallos and Papadopoulos, 2006). As predicted by physicists, environmental challenges, particularly those related to climate change, will occupy a substantial portion of the scientific community's focus in the 21st century.

This marks a historical shift, where environmental problems have become a central priority in scientific research (Kallos and Astitha 2007). Approximately one-third of Earth's terrestrial surface is classified as desert, characterized by aridity, sparse vegetation, and limited precipitation. These landscapes encompass a diverse range of features, including sand dunes, rocky plains, and gravel deposits (Sikoparija, 2020; Jackson, 1996). While plant life may be scarce, they can be present in some desert ecosystems. Mineral deposits, such as salts, are often observed on desert surfaces due to past or ongoing processes of transport and erosion. This erosion is driven by various factors, including thermal fluctuations, frictional interactions between particles of varying sizes, water action, and most importantly, aeolian activity (Adebiyi and Jasper, 2023; Guerzoni and Chester, 1996).

Wind erosion, also known as aeolian activity, represents a significant contributor to atmospheric particulate matter (PM) loads. Aeolian processes mobilize soil dust from desert, arid, and semi-arid regions, transporting these particles over short and long distances. The dynamics of sand transport are primarily influenced by three interrelated factors: particle size, mean wind speed, and turbulent eddies, which play a crucial role in the dispersion and diffusion of sand particles (Eltayeb and Hassan, 1992; Gillette and Ranjit, 1988). The transport of sand is governed by two fundamental modes: saltation and suspension. Saltation involves the hopping motion of medium-sized particles (~100–500 µm), dominating the bed-load transport and accounting for the majority of sand flux through ballistic trajectories and bed impacts (Bagnold, 1941; Kok et al., 2012). In contrast, suspension characterizes the long-distance transport of fine particles (typically < 70 µm), where turbulent eddies overcome gravitational settling, enabling particles to remain aloft for extended periods (Shao, 2008), It can be carried over much longer distances, reaching thousands of kilometers (Rakhesh and Turki, 2024 ; Ndeto and Wekesa, 2023; Waza, 2023). The transition between these modes is critically controlled by particle size, wind velocity, and turbulence intensity, necessitating modeling approaches like the mixture model that adequately resolve the two-phase flow interactions and interphase slip.

A notable example is Saharan dust, which can traverse the Mediterranean Sea in less than a day. The journey across the Atlantic Ocean, however, may take one to two weeks. Annually, approximately 108 tons of Saharan dust are deposited over the Mediterranean waters and a similar quantity is deposited over Europe (Tan and Wang, 2023 ; Gulnura and Kaldybayev, 2023).

Research methodologies in aeolian sand transport involve a diverse array of techniques, including full-scale on-site experiments, full-scale laboratory experiments, reduced-scale laboratory experiments conducted in wind tunnels, and various forms of analytical and semi-empirical modeling (Liu and Zhu, 1998; Liu and Zou, 1994). Additionally, Computational Fluid Dynamics (CFD) is employed for computer simulations to study the phenomena (Westphal and Toon, 1987; Barkan and Kutiel, 2004). Despite the advent of several recent innovative computational fluid dynamics approaches, the Fickian diffusion hypothesis, predicated on turbulent diffusivity, continues to be the predominant framework for studying scalar transport in turbulent flows. The standard gradient diffusion hypothesis necessitates the estimation of the turbulent Schmidt number (Sc), a dimensionless parameter representing the ratio of momentum diffusivity to mass diffusivity in a turbulent flow. Schmidt number is a property intrinsic to both the fluid and the substance being diffused within it (Koeltzsch, 2000 ; Foncubierta and Blázquez, 2023).

Regarding the input data for RANS (Reynolds-Averaged Navier-Stokes)-based approaches, turbulent scalar fluxes are commonly approximated using the standard gradient diffusion hypothesis (SGDH). This hypothesis requires the specification of the turbulent Schmidt number (Sc)(Tominaga and Stathopoulos, 2007; Karimi and Noughabi, 2024). However, there exists a lack of consensus regarding the optimal values for Sc, and standardized computational methods for its determination remain elusive. Numerous studies have been conducted to identify the optimal turbulent Schmidt number (Sc) for numerical simulations of scalar transport in atmospheric systems (Gualtier and Angeloudis, 2017; Wang and Qinpeng, 2023). A subset of these investigations has focused on estimating the most appropriate Sc value and assessing its impact on numerical results. Koeltzsch, (2000) reviewed several previous experimental studies and observed that a majority of researchers employ a constant Sc value within the range of 0.5 to 0.9. Tominaga and Stathopoulos, (2007) conducted a comprehensive review of existing research pertaining to the application of optimal Schmidt numbers (Sc) in engineering flow fields relevant to atmospheric dispersion, including jet-in-cross-flow, plume dispersion in boundary layers, and dispersion around buildings. Their analysis revealed a wide range of optimal Sc values, distributed between 0.2 and 1.3. Notably, the specific Sc value chosen significantly influenced the predictive accuracy of the models.

Given the substantial dependence of optimal Sc values on local flow characteristics, Tominaga and Stathopoulos, (2007) recommended a case-by-case approach to determine Sc. This involves identifying the dominant mechanism of turbulent mass transport in each specific methodes to select an appropriate Sc value. Di Sabatino and Buccolieri, (2007) conducted a comparative analysis of CFD simulations and predictions from a well-established Gaussian model for dispersion in building arrays. Their findings identified optimal Schmidt numbers (Sc) of 0.7 and 0.4 for low and high frontal area densities, respectively. Chavez and Hajra, (2011) executed numerical simulations of pollutant transport in urban environments, encompassing both isolated buildings and building clusters, utilizing Sc values of 0.1, 0.3, and 0.7. Their research demonstrated a significant influence of Sc on CFD simulations of pollutant transport for isolated building configurations.

However, variations in Sc exhibited a lesser impact on assessing pollutant dispersion in the presence of adjacent buildings.

Galeazzo and Donnert, (2013) employed high-resolution measurements using particle image velocimetry and laser-induced fluorescence to validate simulations ranging from simple steady-state RANS to sophisticated LES (Large Eddy Simulation). To enhance the reliability of numerical results, they utilized a constant Sc value within the range of 0.3 to 0.9.

Nevertheless, they emphasized the necessity of considering Schmidt number as a vector quantity (Chen and Wang, 2023). However, the objective of this research is to conduct a thorough investigation of sand particle diffusion within the atmospheric environment. To achieve this goal, we will utilize numerical analysis to examine the influence of the Schmidt number on both dissipation rate and sand particle diffusion coefficient. Furthermore, we will compare the effects of Schmidt number variations on the saltation and suspension modes of aeolian sand transport.

Sand particles transport equations and numerical parameters

The numerical calculations were conducted using the mixture model approach, which tracks the average phase concentration and determines the mixture velocity by solving a single momentum equation (Johansen and Anderson, 1990). The dispersed phase slip velocity, relative to the continuous phase, was calculated based on the equilibrium between body and drag forces arising from the density difference. Governing equations for continuity and momentum were formulated for both the dispersed and continuous phases. Algebraic equations were employed to approximate the momentum equations for the sand particles (Pericleous and Drake, 1986). The modeling was grounded on two fundamental assumptions: both phases occupy the same pressure field, and the density of each phase remains approximately constant. The momentum equation utilized for the mixture model is (Hadjaissa and Salameh, 2023):

$$\rho \mathbf{u}_t + \rho(\mathbf{u}\cdot\nabla)\mathbf{u} = -\nabla p - \nabla\cdot\tau_{Gm} - \nabla\cdot\left[\rho c_d(1-c_d)\left(u_{slip} - \frac{D_{md}\nabla\emptyset_d}{(1-c_d)\emptyset_d}\right)\left(u_{slip} - \frac{D_{md}\nabla\emptyset_d}{(1-c_d)\emptyset_d}\right)^T\right] + \rho g \quad (1)$$

The mass transfer between the two phases can be incorporated by specifying an expression for the mass transfer rate, mdc (kg/(m^3•s)), from the dispersed phase to the continuous phase. The mass transfer rate is generally dependent on the interfacial area between the two phases. The conservation of number density, n (1/m^3), then yields:

$$\frac{\partial n}{\partial t} + \mathbf{j}\cdot\nabla n + \nabla\cdot(n\emptyset_c u_{slip}) = \nabla\cdot(D_{md}\nabla n) - n\, m_{dc}\left(\frac{1}{\rho_c} - \frac{1}{\rho_d}\right) \quad (2)$$

Where j is the volume-averaged velocity.
The interfacial area per unit volume α (m^2/m^3) can be determined by considering the volume fraction of the dispersed particles and the number density :

$$\alpha = (4n\Pi)^{1/3}(3\emptyset_d)^{2/3} \quad (3)$$

In this method, the mixture velocity employed is the mass-averaged mixture velocity, u (m/s). The continuity equation is:

$$(\rho_c - \rho_d)\left\{\nabla\cdot\left[\emptyset_d(1-c_d)u_{slip} - D_{md}\nabla\emptyset_d\right] + \frac{m_{dc}}{\rho_d}\right\} + \rho_c(\nabla\cdot u) = 0 \quad (4)$$

The transport equation for the sand particles (Johansen and Anderson, 1990; Pericleous and Drake, 1986) can be expressed as:

$$\frac{\partial}{\partial t}(\emptyset_d\rho_d) + \nabla\cdot(\emptyset_d\rho_d u_d) = -m_{dc} \quad (5)$$

To validate the applicability of the mixture method in aeolian sand transport studies, the published concentration and velocity profiles of sand particles under analogous experimental conditions (Liu and Dong, 2004) were utilized (Hadjaissa and Salameh, 2023). The computational domain for this investigation was a rectangular wind tunnel measuring 37.8 meters in length with a cross-sectional area of 0.6 square meters. The inlet air velocity, u, was systematically adjusted between 10 and 12 meters per second. To emulate erodible bed conditions, the tunnel floor was uniformly covered with sand. The background turbulence was assumed to be stationary, homogeneous, and isotropic. Two distinct simulation groups were conducted. In the first group, sand particle diameters of D = 2μm (representing

Table 1: *Comparison of numerical approaches for aeolian sand transport modeling*

Method	Advantages	Limitations	Suitability for aeolian transport	References
Mixture Model	Computational efficiency; Handles high particle concentrations; Solves a single momentum equation.	Limited resolution of fine-scale, particle-level interactions.	Excellent for parametric studies and large-scale environmental applications.	Manninen et al. (1996) - On the Mixture Model for Multiphase Flow; Hadjaissa and Salameh (2023) - Application to aeolian sand transport.
Eulerian-Eulerian	Detailed resolution of phase interactions; High accuracy for complex interphase physics (heat/mass transfer).	Computationally intensive; Complex implementation and convergence issues.	Moderate for large-scale simulations due to high computational cost.	Ishii and Hibiki (2011) - Thermo-Fluid Dynamics of Two-Phase Flow; Enwald et al. (1996) - Application to fluidized beds.
Eulerian-Lagrangian	Particle-level tracking (trajectories, history); Very high resolution of discrete particle motion.	Prohibitively expensive for high particle loads (e.g., saltation); Limited to low concentrations.	Poor for dense transport conditions like saltation, but good for dilute suspension.	Maxey and Riley (1983) - Equation of motion for particles; Dehbi (2015) - Application to particle dispersion in turbulence.

suspension transport) were employed. In the second group, sand particle diameters of D = 250 µm (representing saltation transport) were used. For both groups, the Schmidt number was varied from 0.3 to 0.9, while maintaining a constant density of ρ = 2650 kilograms per cubic meter. Given a Mach number below 0.05, air was treated as an incompressible fluid in the absence of sand particles. The outlet pressure was established as a reference value of P_{ref} = 1 atmosphere. Symmetric boundary conditions were applied to both the air and sand phases at the tunnel walls. The governing partial differential equations were discretized using the finite element method (FEM) with a discontinuous Galerkin formulation to enforce boundary conditions. A second-order algorithm was implemented for velocity-pressure coupling.

Results and discussion

Schmidt number and Turbulent diffusion of sand particles

Figures 1 and 2 illustrate the variation of the turbulent diffusion coefficient of sand particles, D_{md} (m/s), with height, z (cm), for various Schmidt number values and both sand diameters, D = 2µm and D = 250µm. As discussed in a previous work (Hadjaissa and Salameh, 2023), this variation can be characterized by a Gaussian function within the boundary layer :

$$D_{md} = a \cdot e^{\left(-\left(\frac{z-b}{c}\right)^2 + a_1 e^{-\left(\frac{z-b_1}{c_1}\right)^2}\right)} \quad (6)$$

Where (a b c), (a1 b1 c1) are terms of the regression results (Hadjaissa and Salameh, 2023).

Figures 1 and 2 demonstrates the influence of Schmidt number values on the diffusion coefficient values. The observed Gaussian distribution of the diffusion coefficient within the boundary layer aligns with previous experimental and numerical studies. For instance, Liu and Dong (2004) reported similar diffusion profiles for sand particles in wind tunnel experiments, while Hadjaissa and Salameh (2023) confirmed this trend using mixture model simulations. The increase in diffusion disparity

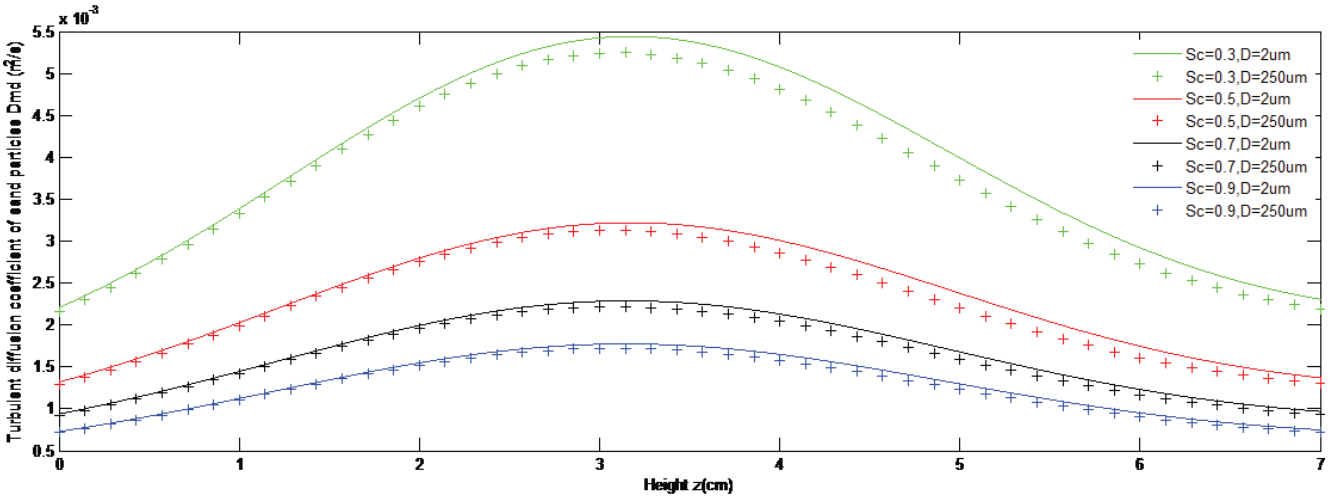

Figure 1: *Vertical diffusion coefficients of sand particles with varying Schmidt number for both sand transport mode within boundary layer (suspension D = 2µm and saltation D = 250µm), U = 10m/s.*

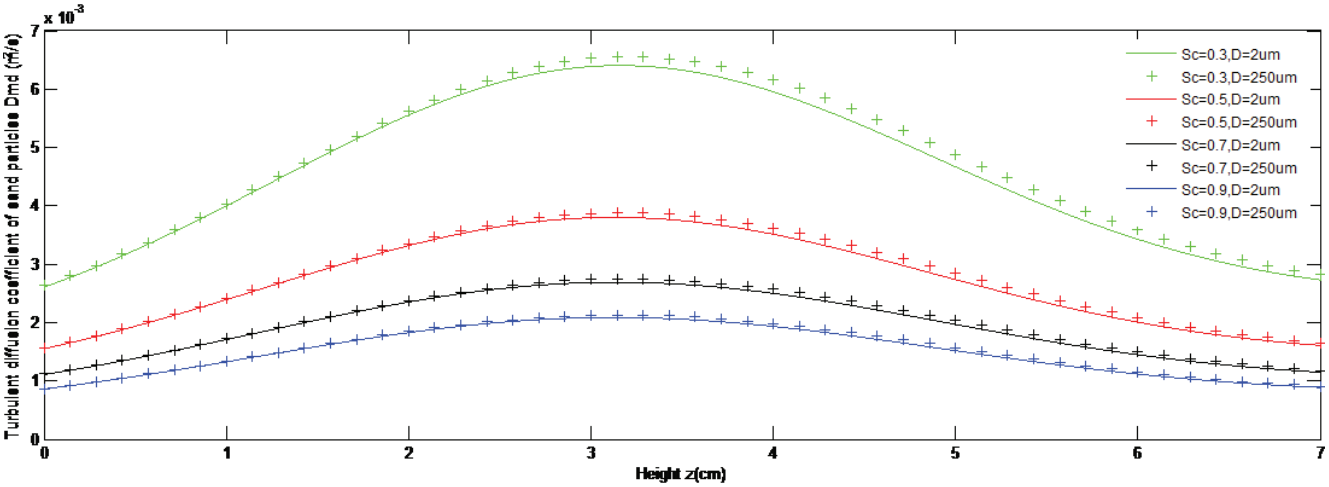

Figure 2: *Vertical diffusion coefficients of sand particles with varying Schmidt number for both sand transport mode within boundary layer (suspension D = 2 µm and saltation D = 250 µm), U = 12m/s.*

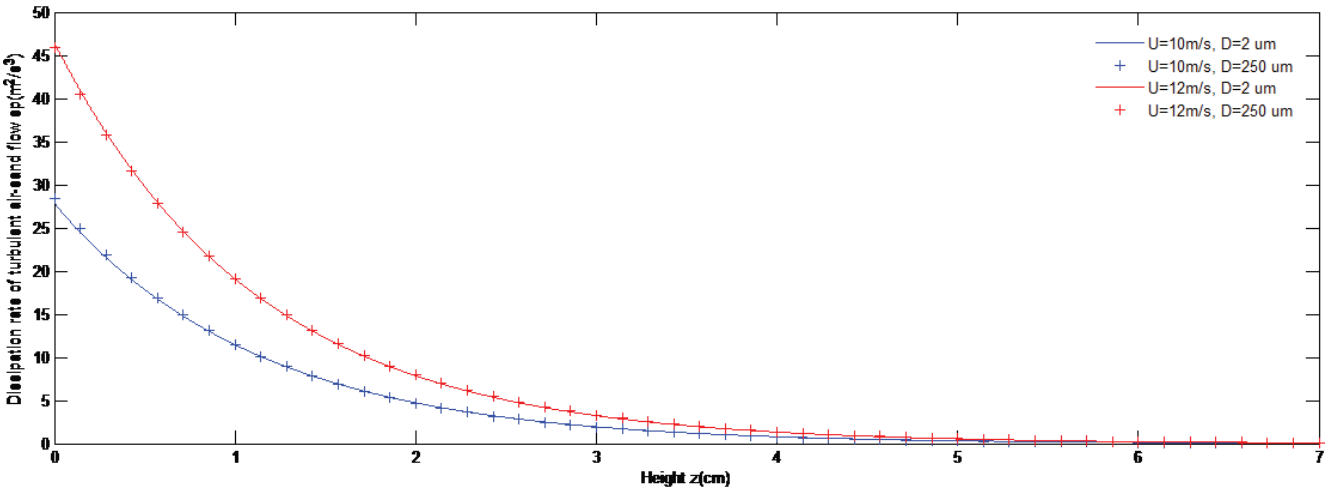

Figure 3: *Vertical dissipation rate of turbulent air-sand flow: Comparative analysis of saltation and suspension modes within boundary layer (D = 2 μm and D = 250 μm, U = 10 m/s and 12 m/s)*

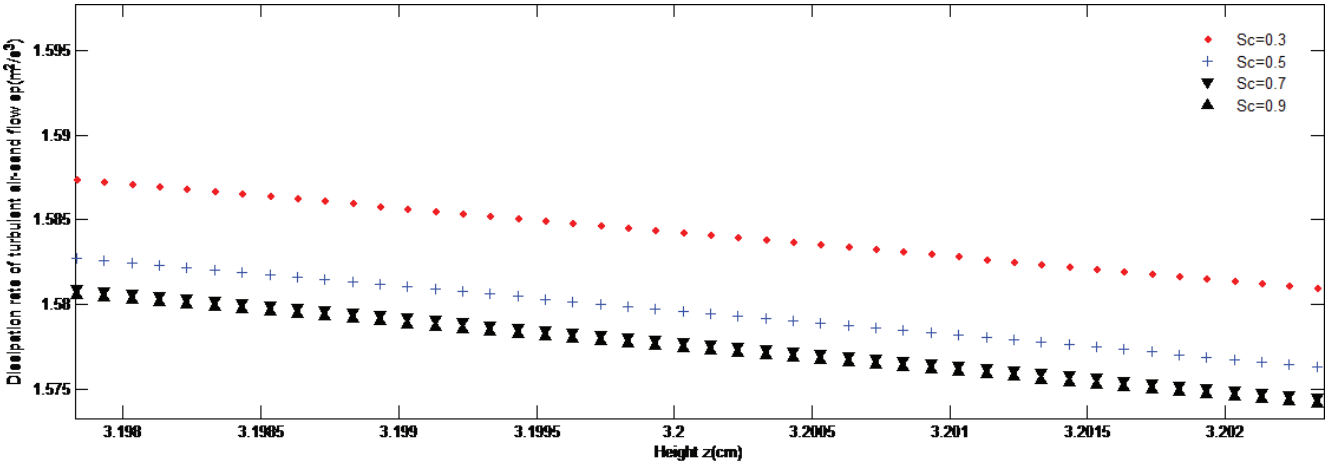

Figure 4: *Vertical dissipation rate of turbulent air-sand flow: Influence of Schmidt number on saltation transport within boundary layer (D = 250 μm, u = 10 m/s)*

near the boundary layer center (z ≈ 3.2 cm) can be attributed to the maximum turbulent kinetic energy in this region, as noted by Koeltzsch (2000) in their analysis of height-dependent Schmidt number effects. This zone fully reveals the inherent differences in particle inertia characterized by the Schmidt number. Low-Schmidt-number particles diffuse vigorously by responding to a wide range of turbulent eddies, whereas high-Schmidt-number particles, being more sluggish, respond poorly, leading to markedly lower diffusion. Thus, the figure confirms that turbulent dispersion is a selective process governed by particle characteristics. At a velocity of 10 m/s, it is observed that sand grains with a smaller diameter, D = 2μm (suspension transport mode), exhibit greater diffusion than sand grains with a medium diameter, D = 250μm (saltation transport mode) (Balachandar and Eaton, 2010). This phenomenon holds true for all Schmidt number values and is attributed to the effect of the grain weight factor, which directly influences the viscosity of the mixture. Conversely, at a velocity of 12 m/s, sand grains with a saltation transport mode demonstrate greater diffusion than sand grains with a suspension mode. The reversal in diffusion dominance between suspension and saltation modes under different velocities (U = 10 m/s vs. 12 m/s) can be explained through particle response time and turbulent eddy interactions. At lower velocities, finer particles (D = 2μm) exhibit higher diffusion due to their ability to follow turbulent fluctuations, consistent with the low Stokes number regime described by Tominaga and Stathopoulos (2007). Conversely, at higher velocities, the increased inertia of saltating particles (D = 250μm) allows them to extract more energy from large-scale eddies, leading to enhanced diffusion—a phenomenon previously observed in particle-laden boundary layers by Wang and Maxey (1993).

Schmidt number and dissipation rate of turbulent air-sand flow

The dissipation rate of turbulent air-sand flow is a crucial parameter in understanding the dynamics of aeolian sand transport. It quantify the rate at which turbulent kinetic energy is converted into internal energy through viscous dissipation. Several factors influence the dissipation rate of turbulent air-sand flow such as shear velocity, particle concentration, bed roughness and particle size. Figure 3 presents a comparative analysis of dissipation rate values for the two sand transport

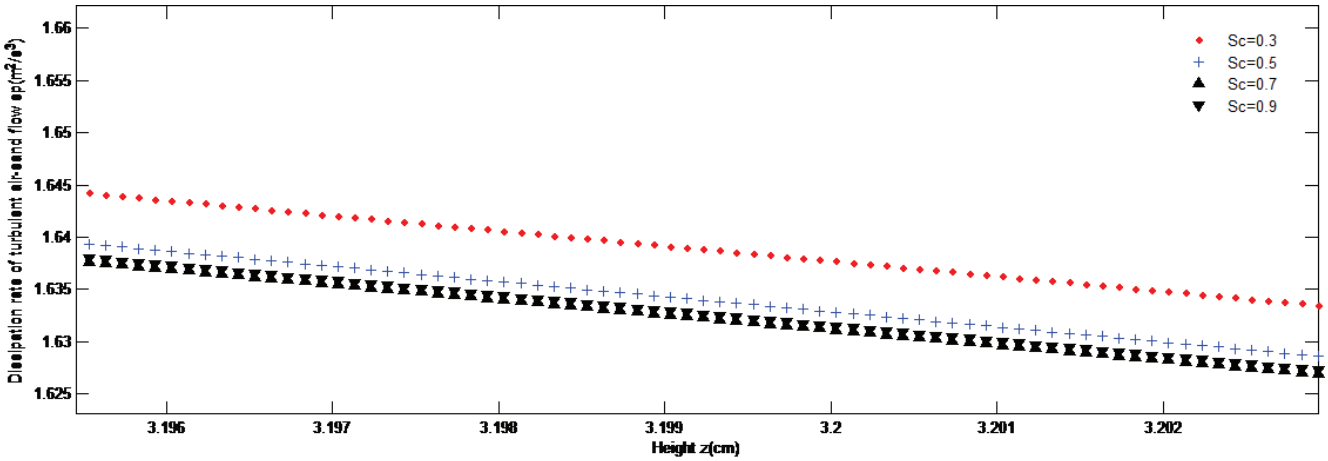

Figure 5: *Vertical dissipation rate of turbulent air-sand flow: Influence of Schmidt number on suspension transport within boundary layer (D = 2 μm, u = 10 m/s)*

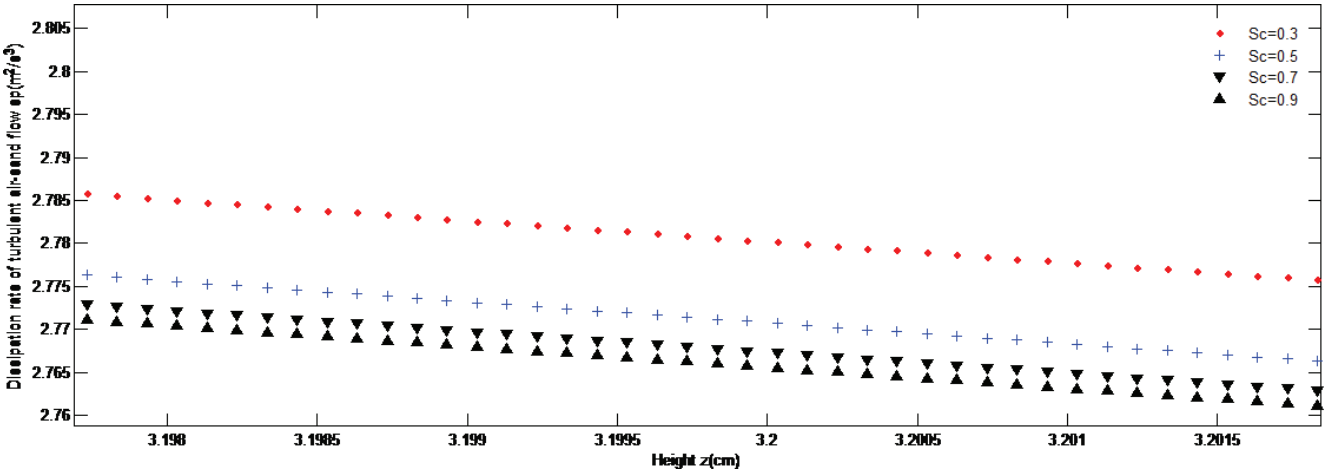

Figure 6: *Vertical dissipation rate of turbulent air-sand flow: Influence of Schmidt number on saltation transport (D = 250 μm, u = 12 m/s)*

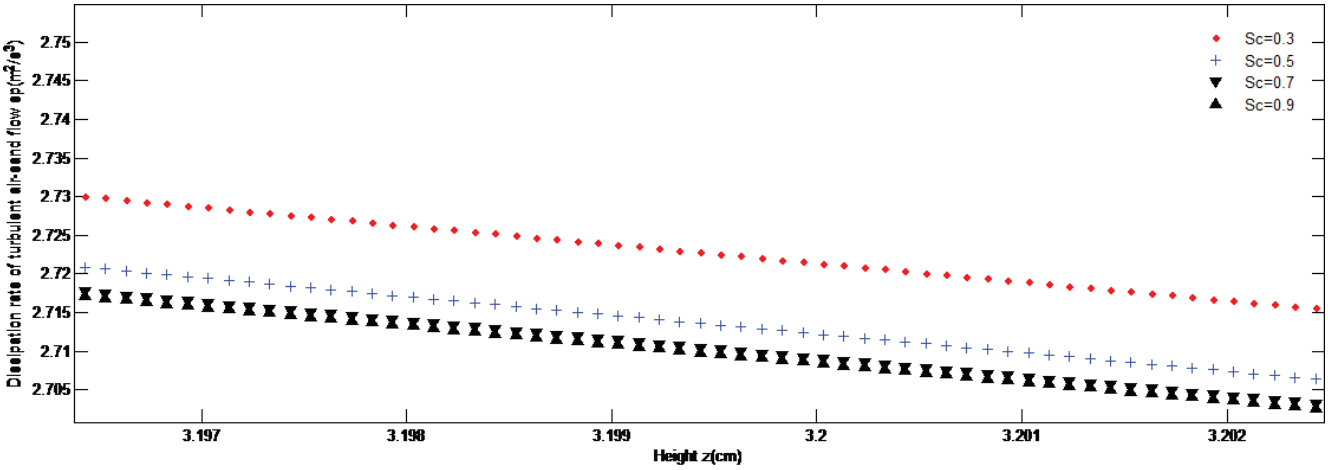

Figure 7: *Vertical dissipation rate of turbulent air-sand flow: Influence of Schmidt number on suspension transport (D = 2μm, u = 12 m/s)*

modes. It is noteworthy that an exponential energy consumption occurs at altitudes proximate to the bed (0 to 4 cm). Although the disparity in dissipation rate values for different Schmidt numbers is not readily discernible in Figure 3, zooming in on the height value of approximately 2.3 cm, which corresponds to the center of the boundary layer zone and the point of maximum diffusion coefficient, reveals the distinction. Figures 4 to 7 depict variations in dissipation rate for different Schmidt number values at two velocities (10 m/s and 12 m/s) and two sand transport modes. The disparity in dissipation rate values for

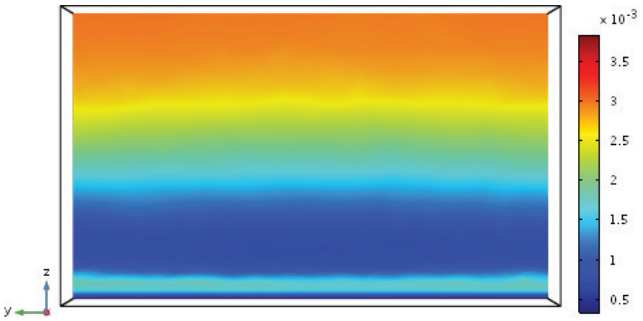

Figure 8: *Spatial distribution of turbulent diffusion coefficient for sand particles in the Z-y plane during saltation transport (D = 250 µm, U = 10 m/s and Sc = 0.7-0.9)*

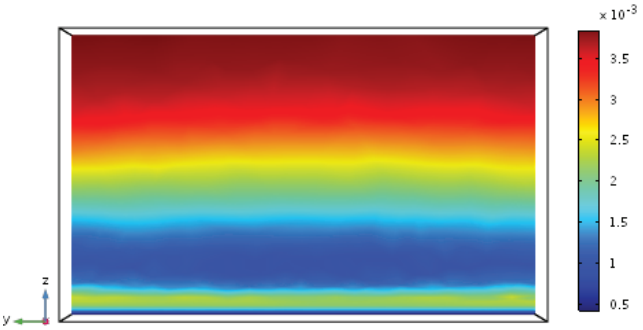

Figure 9: *Spatial distribution of turbulent diffusion coefficient for sand particles in the Z-Y plane during suspension transport (D = 2 µm, U = 10 m/s and Sc = 0.7-0.9)*

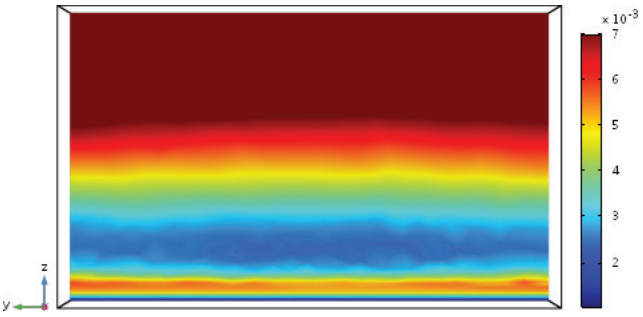

Figure 10: *Spatial distribution of turbulent diffusion coefficient for sand particles in the Z-Y plane during suspension transport (D = 2 µm, U = 10 m/s and Sc = 0.3)*

varying Schmidt coefficient values is observable. It is noteworthy that convergence occurs in the results between the Schmidt coefficient values of 0.7 and 0.9, suggesting that the variation in relative rates of momentum diffusion and mass diffusion within a fluid has a minimal impact on the turbulence structure within the range of 0.7 to 0.9. The relationship between dissipation rate and Schmidt number in aeolian sand transport is not directly analogous to the diffusion coefficient of particles. It is noteworthy that setting Schmidt values close to unity at the inlet data does not necessarily result in the convergence of consumed energy values in this interval. This convergence can be interpreted as an indicator of the stability of the turbulence structure within the field of 0.7 to 0.9 for the sand-air mixture in the phenomenon of the aeolian sand transport which corresponds to (Tominaga and Stathopoulos, 2007; Koeltzsch, 2000) works. This convergence is more pronounced in suspension mode compared to saltation mode.

Spatial distribution of turbulent diffusion coefficient

Figure 8 and 9 illustrate the spatial sand diffusion coefficient, Dmd (y, z), within the y-z plane for converged Schmidt numbers of 0.7 to 0.9. These simulations were conducted at a wind velocity of u = 10 m/s and particle diameters of D = 2µm and D = 250µm respectively, in the working section of the wind tunnel (1 m x 0.6 m, x = 10 m to inlet). Both figures provide insights into the distinct diffusion patterns of sand grains during saltation and suspension transport. In the boundary layer region, extending from the bed to approximately 7 cm vertically, a pronounced increase followed by a rapid decrease in Dmd is observed. This trend aligns with previous findings. Above the boundary layer, a region of relatively low diffusion (blue region) is evident, extending to a height of approximately 10 cm to 50 cm. Beyond this region, Dmd gradually increases towards the upper limits of the tunnel. Notably, sand grains in suspension transport exhibit a more diffused distribution compared to those in saltation transport, likely due to their larger size.

Figure 10 illustrates the spatial sand diffusion coefficient, Dmd on the Y-Z plane for a Schmidt number (Sc) of 0.3, an air velocity u = 10 m/s, and a particle diameter D = 2µm. Figure 9 and 10 were obtained under identical conditions of wind speed and sand grain diameter, with the distinction residing in the Schmidt number 0.7 and 0.3 respectively. A significant disparity is observed between the two figures. The maximum value of the sand particle diffusion coefficient is 3.5×10^{-3} in Figure 9 and 7×10^{-3} in Figure 10, respectively, within the tunnel limits. This discrepancy underscores the necessity of exercising caution in selecting the Schmidt number when simulating natural phenomena involving the transport of solid bodies by fluids, such as the Aeolian sand transport.

Table 2: *Comparative analysis of saltation and suspension transport modes*

Parameter	Saltation (D = 250 µm)	Suspension (D = 2 µm)	References
Dominant diffusion mechanism	Particle inertia-driven	Turbulent fluctuation-driven	Tominaga and Stathopoulos (2007)
Sensitivity to Sc variations	Moderate	High	Current Study
Typical transport height	< 1 m	> 10 m	Liu and Dong (2004)
Impact on air quality	Localized PM_{10} emissions	Long-range $PM_{2.5}$ transport	Ndeto and Wekesa (2023)

Conclusion

This study systematically investigated the role of the turbulent Schmidt number in aeolian sand transport dynamics through comprehensive mixture model simulations. Our analysis reveals three key findings:

First, we identified a stable convergence range (Sc = 0.7–0.9) where turbulent dissipation rates become insensitive to Schmidt number variations across both saltation and suspension transport modes. This finding challenges the conventional practice of using fixed Sc values and provides empirical support for the optimal range suggested by Tominaga and Stathopoulos (2007).

Second, our results demonstrate the dual dependence of particle diffusion on both grain size and wind velocity. The reversal in diffusion dominance between suspension and saltation modes at different velocities (10 m/s vs. 12 m/s) reveals complex particle–turbulence interactions that were not fully captured in previous studies such as Liu and Dong (2004).

Third, the spatial distribution analysis clearly shows that Schmidt number selection critically influences diffusion pattern predictions, with Sc = 0.3 producing significantly different results than Sc = 0.7–0.9.

The primary contribution of this work lies in establishing a physically justified framework for Schmidt number selection in aeolian transport modeling. By identifying the 0.7–0.9 range as a stability threshold, our study provides:

- Improved parameterization of dust emission in climate models using scenario-dependent Schmidt numbers.
- More accurate prediction of PM_{10} and $PM_{2.5}$ dispersion from arid regions, supporting early warning systems for dust storms.
- A reference standard for future CFD studies of particle-laden atmospheric flows.

These findings advance the field beyond the empirical approaches reviewed by Koeltzsch (2000) and provide a mechanistic basis for optimizing the turbulent Schmidt number in environmental flow simulations. Future research should focus on incorporating variable Sc values in advanced CFD models, accounting for terrain complexity and atmospheric stratification. By clarifying the critical role of Sc, this study contributes to more reliable and physically consistent models of aeolian sand transport under changing climatic conditions.

References

Adebiyi, A. and Jasper, K., A review of coarse mineral dust in the Earth system. Aeolian Research Volume 60, 2023. 100849. https://doi.org/10.1016/j.aeolia.2022.100849

Barkan, J. and Kutiel, H. and Alpert, P., Climatology of Dust Sources in North Africa and the Arabian Peninsula, Based on TOMS Data. Indoor and Built Environment, Volume 13, Issue 6 pp.13:407–419.2004. https://doi.org/10.1177/1420326X04046935

Balachandar, S. and Eaton, K., Turbulent Dispersed Multiphase Flow. Annu. Rev. Fluid Mech. 2010. 42:111–33.

Bagnold, R.A,The Physics of Blown Sand and Desert Dunes. Methuen, London. 1941.

Chavez, M. and Hajra, B. and Stathopoulos, T. and Bahloul, A., Near-field pollutant dispersion in the built environment by CFD and wind tunnel simulations. J. Wind Eng. Ind. Aerodyn., 99, 330–339, 2011.

Chen, J. and Wang, D., Numerical simulations of mass transfer in turbulent pipe flow at high schmidt numbers. Heat and Mass Transfer, Volume 59, pages 1333–1341, (2023).

Dehbi, A. A Eulerian-Lagrangian model for dense particle clouds using a statistical parcel method.

Computers & Fluids, (2015). 113, 68-79. https://doi.org/10.1016/j.compfluid.2015.02.008

Di Sabatino, S. and Buccolieri, S., Experiment simulations using CFD and integral models. In Proceedings of the 11th International Conference on Harmonisation within Atmospheric Dispersion Modelling for Regulatory Purpose, Cambridge, UK, 2–5 July 2007.

Enwald, H., and Peirano, E., and Almstedt, A. Eulerian two-phase flow theory applied to fluidization. International Journal of Multiphase Flow, (1996). 22, 21-66. https://doi.org/10.1016/S0301-9322(96)90004-X

Eltayeb, I. and Hassan, M., Two-dimensional transport of dust from an infinite line source at ground level. Geophysical Journal International, Volume 110, Issue 3, Pages 571–576, 1992, https://doi.org/10.1111/j.1365-246X.1992.tb02092.x

Foncubierta, J. and Blázquez, I., Maestre Experimental adjustment of the turbulent Schmidt number to model the evaporation rate of swimming pools in CFD programmes Case Studies in Thermal Engineering, Vol 4, 2023. https://doi.org/10.1016/j.csite.2022.102665

Galeazzo, F. and Donnert, G., Computational modeling of turbulent mixing in a jet in crossflow, International Journal of Heat and Fluid Flow,Volume 41, 2013. https://doi.org/10.1016/j.ijheatfluidflow.2013.03.012.

Gillette, A. and Ranjit, P., Modeling dust emission caused by wind erosion, Journal of Geophysical Research: Atmospheres, Volume 93, Issue D11, Pages 14233-14242. 1988.

Guerzoni, S. and Chester, R., The Impact of Desert Dust Across the Mediterranean, Environmental Science and Technology Library ENST, Volume 11. ISBN 978-90-481-4764-9. 1996.

Gulnura, I. and Kaldybayev, A., Spatial and Temporal Characteristics of Dust Storms and Aeolian Processes in the Southern Balkash Deserts in Kazakhstan, Central Asia. Land, 12(3), 668, 2023. https://doi.org/10.3390/land12030668

Hadjaissa, A. and Salameh, T., Concentration and turbulent diffusivity of sand particles in the atmosphere based on mixture model theory, International Journal of Fluid Mechanics Research, Vol.50, Issue 3, pp. 17-31, 2023. https://doi.org/10.1615/InterJFluidMechRes.2023045217

Ishii, M., and Hibiki, T. Thermo-Fluid Dynamics of Two-Phase Flow (2nd ed.). (2011) Springer. https://doi.org/10.1007/978-1-4419-7985-8

Jackson, D., Potential inertial effects in Aeolian sand transport: preliminary results, Sedimentary Geology, 106, pp. 193–201. 1996.

Johansen, S. and Anderson, N. and De Silva, S., A two-phase model for particle local equilibrium applied to air classification of powers, Power Technology, Vol. 63, pp. 121 – 132, 1990.

Kallos, G. and Astitha, M. and Katsafados, P. and Spyrou, C., Long-Range Transport of Anthropogenically and Naturally Produced PM in the Mediterranean and North Atlantic: Present Status of Knowledge, Journal of Applied Meteorology and Climatology, Volume 46: Issue 8, Page(s): 1230–1251. 2007.

Kallos, G. and Papadopoulos, A. and Katsafados, P. and Nickovic, S., Trans-Atlantic Saharan dust transport: Model simulation and results. Journal of Geophysical Research Atmosphere, Volume111, IssueD9, 2006. https://doi.org/10.1029/2005JD006207.

Koeltzsch, K., The height dependence of the turbulent Schmidt number within the boundary layer. Atmos. Environ., 34, 1147–1151.2000.

Kok, J.F., Parteli, E.J.R., Michaels, T.I. and Karam, D.B. The physics of wind-blown sand and dust. Reports on Progress in Physics, 2012,75(10), p.106901. https://doi.org/10.1088/0034-4885/75/10/106901

Liu, X. and Dong, Z., Experimental investigation of the concentration profile of a blowing sand cloud, J.Geomorphology 60. 371–381,2004.

Liu, Z. and Zhu, J. and Kuang, Z., Saltation in windblown sand, Sci. China Ser. A-Math. 41, 629–637, 1998. https://doi.org/10.1007/BF02876233

Liu, Z. and Zou, J. and Dong X., Tentative calculation of wind–sand current energy, Chin. Sci. Bull. 39, 1016–1020, 1994.

Manninen, M., and Taivassalo, V., and Kallio, S. On the Mixture Model for Multiphase Flow. VTT Publications 288. (1996). Technical Research Centre of Finland (VTT).

Maxey, M. and Riley, J., Equation of motion for a small rigid sphere in a nonuniform flow. The Physics of Fluids, (1983). 26(4), 883–889.

Ndeto, M., and Wekesa, D., Aeolian dust distribution, elemental concentration, characteristics and its effects on the conversion efficiency of crystalline silicon solar cells Renewable Energy Volume 208., Pages 481-491. 2023. https://doi.org/10.1016/j.renene.2023.03.065

Pericleous, K. and Drake, S., An Algebraic Slip Model of PHOENICS for Multi-phase Applications, Numerical Simulation of Fluid Flow and Heat/Mass Transfer Processes Lecture Notes in Engineering vol 18. Springer, Berlin, Heidelberg, 1986. https://doi.org/10.1007/978-3-642-82781-5-29

Rakhesh, M. and Turki, A. Aeolian dust and hydro-biological characteristics: Decoding dust storm impacts on phytoplankton in the northern Arabian Gulf. Science of The Total Environment. Volume 911, 2024. 168583. https://doi.org/10.1016/j.scitotenv.2023.168583

Seinfeld, J. and Pandis, S., Atmospheric Chemistry and Physics: From Air Pollution to Climate Change, New York: Wiley-Interscience, ISBN 0471178160. 1997.

Sikoparija, B., Desert dust has a notable impact on aerobiological measurements in Europe Aeolian Research Volume 47, 2020. 100636. https://doi.org/10.1016/j.aeolia.2020.100636

Shao, Y., Physics and Modelling of Wind Erosion (2nd ed.). Springer, Dordrecht. 2008.

Tominaga, Y. and Stathopoulos, T., Turbulent Schmidt numbers for CFD analysis with various types of flowfield. Atmos. Environ., Vol 41, 8091–8099. 2007.

Tan, L. and Wang, H., Aeolian sand transport over a dry playa surface: Sand flux density profiles, saltation layer height, and flux scaling laws and implications for dust emission dynamics, CATENA, Volume 224, 2023. https://doi.org/10.1016/j.catena.2023.106970

Wang, L. and Maxey, M., Settling velocity and concentration distribution of heavy particles in homogeneous isotropic turbulence. Journal of Fluid Mechanics, Volume 256 ,1993, pp. 27 – 68.

Wang, D., Numerical simulations of mass transfer in turbulent pipe flow at high schmidt numbers. Heat and Mass Transfer, Vol 59, pages 1333–1341, 2023.

Wang, X. and Santos Ferreira, C., Studying the function of ecosystem in preventing aeolian dust emission in the dryland areas of China. European Journal of Soil Science. Volume 74, Issue 3 - e13371. 2023. https://doi.org/10.1111/ejss.13371

Wang, F. and Qinpeng, M.,The Turbulent Schmidt Number for Transient Contaminant Dispersion in a Large Ventilated Room Using a Realizable k-ε Model, Fluid Dynamics & Materials Processing, 20(4), 829-846, 2024. https://doi.org/10.32604/fdmp.2023.026917

Waza, A. and Kjer, J., Aeolian dust resuspension on Mars studied using a recirculating environmental wind tunnel. Planetary and Space Science,Volume 227, 2023, 105638.

Westphal, D. and Toon, O. and Carlson, T., A two-dimensional numerical investigation of the dynamics and microphysics of Saharan dust storms, Journal of Geophysical Research, 92, pp. 3027–3049. 1987.